DNA methylation plays a role on *in vitro* culture induced loss of virulence in *Botrytis cinerea*

James Breen[1,2], Luis Alejandro Jose Mur[3], Anushen Sivakumaran[3], Aderemi Akinyemi[3], Michael James Wilkinson[3], Carlos Marcelino Rodriguez Lopez[4*]

[1]Robinson Research Institute, University of Adelaide, Adelaide SA 5005

[2]University of Adelaide Bioinformatics Hub, School of Biological Sciences, University of Adelaide, Adelaide SA 5005

[3]Pwllpeiran Upland Research Centre, Institute of Biological, Environmental and Rural Sciences, Edward Llywd Building, Penglais Campus, Aberystwyth, Ceredigion, SY23 3FG, UK.

[4]Environmental Epigenetics and Genetics Group, School of Agriculture, Food and Wine, Waite Research Precinct, University of Adelaide, PMB 1, Glen Osmond, SA 5064, Australia.

Corresponding author

Abstract

Pathogenic fungi can lose virulence after protracted periods of culture but little is known of the mechanisms regulating this. Here we assess whether DNA methylation could play a role in this phenomenon by the methylome analysis of virulent and reduced virulence derivative cultures of *Botrytis cinerea*, and identify the genes/genomic regions affected by these epigenetic modifications. Virulence declined during the eight months culture and recovered after one fungal generation on *A. thaliana*. Methylation-sensitive amplified polymorphisms show that epi/genetic variation followed virulence changes during culture. Whole genome sequencing showed no significant genetic changes during culture. Conversely, bisulfite sequencing showed significant changes both on global and local methylation patterns. We suggest that virulence is a non-essential plastic character regulated by DNA methylation during protracted *in vitro* culture. We propose DNA methylation as a regulator of the high virulence/low virulence transition in *B. cinerea* and as a potential mechanism to control pathogenicity.

Introduction

Botrytis cinerea is a pathogenic ascomycete responsible for grey mould on hundreds of dicotyledonous plant species and is able to feed on many different plant tissue types (1). It is estimated that the disease causes annual losses of up to $100 billion worldwide (2). The wide variety of host tissues and species implies that *B. cinerea* is highly plastic in host specificity with a large 'arsenal of weapons' at its disposal. *B. cinerea* is well documented to be a capable saprotroph and necrotroph with genetic types showing a trade-off between saprotrophic and necrotrophic capabilities (3). As with other pathogens, *B. cinerea* undergoes transcriptional and developmental regulation to govern the outcome of interactions with its host plants. However, changes in virulence levels are not under strict developmental control

and have, for example, also been observed to alter during protracted *in vitro* culture of *B. cinerea* (4). In fact, pathogenic fungi are notorious for losing virulence when successively subcultured *in vitro*. Degenerated cultures of this kind have been reported in a wide range of pathogenic fungi (5) but very little is known about why cultures degenerate in virulence. Different factors have been described as possible causes of the observed loss of virulence during culture including dsRNA mycoviruses (6,7), loss of conditional dispensable chromosomes (8,9) or culture-induced selection of nonvirulent strains. However, one characteristic common to almost all *in vitro*-derived non-virulent fungal strains is that their virulence is restored after one passage on their host (5). If attenuated strains recover virulence, then loss of virulence cannot be explained by mycoviruses infection or chromosome loss. Furthermore, fungal strains in culture lose virulence irrespective of whether the parent culture was derived from a single spore or multi-spore colony (5), suggesting that there cannot be a culture induced selection of nonvirulent strains.

The reversibility of this aspect of the observed phenotype comes in response to changes in the growing environment and so could be viewed as phenotypic plasticity (10). In 1942 C.H. Waddington (11) first proposed the term epigenotype to describe the interface between genotype and phenotype. Since then, a large body of research has been carried out to better understand the role of epigenetic regulatory systems in shaping the phenotype of higher organisms surviving in fluctuating environments (12,13). Epigenetic processes operate in a number of ways to alter the phenotype without altering the genetic code (14). These include DNA methylation, histone modifications, and mRNA editing and degradation by noncoding RNAs. Such processes are intimately entwined and often work in a synergistic way to ultimately achieve changes in phenotype (15). DNA methylation, and more specifically cytosine methylation (i.e. the incorporation of a methyl group to carbon 5 of the cytosine

pyrimidine ring to form 5-methylcytosine (5-mC)) is the most studied epigenetic mechanism. It is present across many eukaryotic phyla, including plants, mammals, birds, fish, and invertebrates and provides an important source of epigenetic control for gene expression (16). In plants and animals, DNA methylation is known to be involved in diverse processes including transposon silencing, X-chromosome inactivation, and imprinting (17). In fungi, several studies have showed changes in overall 5-mC content during development in *Phymatotrichu omnivorum* (18) and *Magnaporthe oryzae* (19). Global patterns in DNA methylation has been previously shown to dramatically change in lichen fungi species when exposed to the algal symbiont (20). Whole-methylome sequencing in Ascomycetes has shown that this group of fungi present heavily methylated silent repeated loci and methylated active genes. Zemach et al, (21) reported a correlation between gene body methylation and *gene* expression levels in *Uncinocarpus reesii*. More recently, Jeon et al., (19) ascribed a developmental role for DNA methylation in *M. oryzae.* In this pivotal paper, it was demonstrated that DNA methylation density in and around genes changes during development, and that transcript abundance is negatively affected by DNA methylation upstream and downstream of ORFs while gene body methylation is linked to enhanced expression. Recent years have seen a dramatic increase in the depth of understanding of how epigenetic control mechanisms operate during plant/pathogen interactions (2,22). However, little is known of the possible role played by DNA methylation processes related to virulence in fungal plant-pathogen interactions. The authors are specifically aware of no studies describing DNA methylation dynamics associated with protracted periods of culture and the associated loss of virulence from a pathogenic fungus. In this paper, we seek to explore possible links between erosion of pathogenicity from *B. cinerea* during protracted *in vitro* culture and dynamics of DNA methylation across their genomes. We used Methylation Sensitive Amplified Polymorphisms (MSAPs) (23) to provide a preliminary survey of

96 methylome flux associated with gradual changes to *B. cinerea* pathogenicity that occurs
97 during protracted *in vitro* culture. We next sought to identify candidate regions whose change
98 in methylation status may be specifically associated with loss of virulence. For this, we
99 identified Differentially Methylated Regions (DMRs) associated to the loss of pathogenicity
100 during *in vitro* culture using sodium bisulfite whole genome sequencing of from different
101 times in culture.

102

103 **Results**

104 **Pathogenicity analysis of *Botrytis cinerea***

105 All isolates obtained from all culture time points produced lesions on *A. thaliana* but they
106 varied in their severity (Figure 1A). As *B. cinerea* was successively cultured, the disease
107 scores imposed by each inoculation progressively decreased over the eight-month period,
108 denoted as time 0 to time 8 months (i.e. T0-T8) (Figure 1B). The apparent loss of virulence
109 with time in culture becomes significant from 3 months (T3) onwards (T-Test $P< 0.05$)
110 (Figure 1B). The disease scores for the T8P challenge did not differ significantly from those
111 for those at T0 culture time, suggesting that virulence had recovered following a single
112 passage through a plant (Figure 1B). Conversely, T8 virulence scores were significantly
113 lower than those obtained from T0 to T5 and also than T8P (T-Test $P< 0.05$) (Figure 1B).
114 Fungal DNA content within the infected areas of the leaf was measured by quantitative PCR
115 (24) to confirm that *in planta* fungal growth was greater using inoculum from time points T0
116 and T8P than from T8. Infected leaves with T0 and T8P cultures did not show significant
117 differences in fungal DNA content (Figure 1C). However, both showed significantly higher
118 levels of fungal DNA (T-Test $P< 0.05$) when compared to those infected using T8 cultures
119 (Figure 1C).

120

121 **Analysis of genetic and epigenetic variance during culture using MSAPs**

122 MSAP profiles generated a total of 74 loci (22 unique to *Hpa*II, 4 unique to *Msp*I and 48
123 common to both restriction enzymes) for the 112 samples of eight *B. cinerea* culture times
124 used in this study (T2-T8P). Multivariate analysis of the MSAP profiles revealed that the
125 global methylation profiles of *B. cinerea* became progressively more dissimilar to the first
126 time point analysed (T2) with increasing culture age (Figure 2). Both, PCoA (Figure 2A and
127 C) and PhiPT values (Figure 2B) showed higher levels of culture-induced variability when
128 using *Hpa*II than when using *Msp*I. PCoA shows that samples cultivated for 3, 4, 5, 6, and 7
129 months occupied intermediate Eigenspace between samples cultivated for 2 and 8 months
130 (Figure 2C). Furthermore, a partial recovery of the MSAP profile was observed on samples
131 cultured for 8 months after one fungal generation on the host plant (T8P) (Figure 2C).
132 Calculated PhiPT values between each time point and T2 samples show a progressive
133 increase in methylome distance with time in culture when samples were restricted with both
134 enzymes. Analysis of Molecular Variance (AMOVA) analysis shows that the calculated
135 PhiPT values were significantly different ($P<0.05$) between T2 and time points T6, T7, T8
136 and T8P when using *Msp*I and T7, T8 and T8P when using *Hpa*II (Figure 2B). Mantle test
137 analysis showed significant correlations between changes in virulence between culture time
138 points and the pairwise distances calculated from MSAP profiles generated using *Msp*I (R^2 =
139 0.316; P=0.005) and *Hpa*II (R^2 = 0.462; P=0.002) (Figure S1).

140

141 ***B. cinerea* genome resequencing**

142 To determine if the *in vitro* culture variability detected using MSAP analysis could be
143 attributed to genetic changes, pooled, sequenced and compared DNA extractions from 3

144 independent cultures from two time points (1 month (T1) and 8 months (T8) in culture) to the
145 Broad Institute's *B. cinerea* B05.10 reference genome sequence
146 (http://www.broadinstitute.org/scientific-community/science/projects/fungal-genome-
147 initiative/botrytis-cinerea-genome-project). Both samples were sequenced to an average
148 depth of 37.47x (35.64x for the 1-month culture and 39.30x for the 8-month culture) with an
149 average of 80% of reference bases being sequenced to a depth greater than 10x. After
150 filtering for coverage greater than 10x and >30 variant quality, 186,275 variants were
151 identified compared to the B05.10 reference, with 174,456 variants being shared between
152 both time points (i.e. T1 = T8). Additional filtering was used to remove multi-allelic variants,
153 variants with missing data in one sample and variants with an observed allele frequency less
154 than 0.5 (25). This filtering reduced the number of non-shared variants to 2,331, of which
155 1,030 (44%) were small insertions and deletions (INDELs) and 1,301 (56%) SNPs. Of the
156 2,331 filtered variants analysed, 454 were located within genes including: 251 synonymous
157 variants, 198 non-synonymous mutations (193 causing missense variations and 5 causing
158 premature stop codons (non-sense mutations) all located in genes with unknown functions
159 (BC1G_07064, BC1G_08869, BC1G_08189, BC1G_12710 and BC1G_01150). An
160 additional 5 variants that altered predicted splice junctions were also identified.

161 We next focused the search for variants within the sequence of 1,577 *B. cinerea* genes with
162 known function including: secondary metabolism (i.e. sesquiterpenecyclases,
163 diterpenecyclases, paxillin-like enzymes, fusiccocin-like enzymes, Phytoene synthases, non-
164 ribosomal peptide synthetases, polyketides synthases, chalcone synthases, DiMethylAllyl
165 Tryptophan Synthases) (26), conidiation (26), sclerotium formation (25), mating and fruit
166 body development (26), apoptosis (26), housekeeping (26), signalling pathways (G protein-
167 coupled receptors, MAP kinases, heterotrimeric G proteins, cAMP signalling components
168 and Ca^{2+}-related signalling) (26) and virulence *senso lato* genes (147 genes were duplicated,

169 i.e., present in more than one category). The virulence *sensu lato* genes included: 12
170 appressorium-associated genes (26), 17 virulence *sensu stricto* genes (27) and 1,155 plant cell
171 wall disassembly genes (CAZyme genes) (28). Of the 1,577 tested genes, 68 (4.3%)
172 contained one or more variants between T1 and T8 (See Table 1 and Supplementary Table 1
173 for a comprehensive list of genes with variants).

174

175 **Characterisation of DNA Methylation changes by whole-genome bisulfite sequencing**

176 To validate and better characterise the DNA methylation changes observed during culture of
177 *B. cinerea* using MSAP analysis, we generated genome-wide DNA methylation maps across
178 the fungal genome by conducting whole-genome bisulphite sequencing (WGBS) from
179 triplicated genomic DNA extractions from mycelia of two different culture ages (T1 and T8)
180 and from samples culture for eight months and then inoculated onto an *A. thaliana* plant
181 (T8P). WGBS of these samples yielded 187.5 million reads ranging from 12.61 to 34.05Gbp
182 per sample after quality filtering. Mapping efficiency of each replicate ranged from 54.3 to
183 67.6%, resulting in samples that generated between 33 and 55x coverage of the 42.66Mbp
184 genome (Supplementary Table 2). This is the highest genome coverage achieved to date for
185 any fungal species after bisulfite sequencing. On each sample, we covered over 91-93% of all
186 cytosines present in the genome (Supplementary Table 2), with all samples having at least
187 81% of cytosines covered by at least four sequencing reads, allowing methylation level of
188 individual sites to be estimated with reasonable confidence.

189

190 Bisulfite sequencing identified an average of 15,716,603 mC per sample, indicating an
191 average methylation level of 0.6% across the genome as a whole, with varying levels in
192 individual samples (Supplementary Table 2). The most heavily methylated context was CHH

193 followed by CG and CHG (where H is A, C or T) (Supplementary Table 3). Although global
194 levels of mC did not significantly change with culture time, methylation in the rarer CG and
195 CHG contexts increased significantly (T-test, p=0.0008 and 0.0018) between 1 and 8 months
196 in culture (Figure 3A). Both types of methylation showed a decreasing trend (not significant)
197 on samples recovered from eight month old cultures inoculated onto *A. thaliana* (T8P)
198 (Figure 3A). Analysis of local levels of DNA methylation across the largest *B. cinerea* contig
199 (Supercontig 1.1) showed that DNA methylation is not evenly distributed but locally
200 clustered (Figure 3B-D). Observed clustering patterns were similar in all analysed samples
201 (Figure 3B-D).

202

203 We next investigated the fine distribution of DNA methylation across genic and regulatory
204 regions by surveying the location and density of mCs on all B. cinerea genes (exons and
205 introns), and promoter regions, defined here as 1.5 kb upstream of the Transcription Starting
206 Site (TSS). Among these, mC levels increased between 1,000 and 500bp upstream of TSS.
207 This was followed by a sharp decrease and increase in methylation before and after the start
208 of the coding sequence (Figure 4). When the different time points were compared for these
209 same global methylation levels where higher on T8P samples (Figure 4), in parallel with that
210 observed at a whole-genome level (Figure 3A).

211

212 The same methylation density analysis was then carried out for five loci corresponding to
213 four housekeeping genes in Botrytis (i.e., G3PDH (Glyceraldehyde 3-phosphate
214 dehydrogenase) (BC1G_09523.1); HSP60 (Heat Shock Protein 60) (BC1G_09341.1); Actin
215 (BC1G_08198.1 and BC1G_01381.1) and Beta Tubulin (BC1G_00122.1). All five Loci

present low levels of DNA methylation in every context and no changes in DNA methylation were observed between time points (i.e., T1, T8 and T8P) (Data not shown).

Finally, methylation density was analysed on 131 genes encoding putative CAZymes secreted by *B. cinerea* upon plant infection (Supplementary Table 4) (28). As a whole, these genes showed the same methylation pattern as described above for all *B. cinerea* genes with an increase in methylation upstream of the TSS (Figure 5A). More interestingly, these genes showed higher levels of methylation after 8 months in culture than at T1 and at T8P. This observed increase in global methylation on T8 samples was due to an increase on the CHG and CG (Figure 5B-C) contexts. Conversely, CHH (Figure 5D) showed higher levels of methylation on the T8P samples, following the general trend observed both at a whole genome level (Figure 3A) and by all *B. cinerea* genes (Figure 4).

Detection of culture induced DMRs

We sought to identify loci exhibiting DMRs between culture times (T1, T8 and T8P) by comparing methylation levels across the whole genome of all samples using a sliding window analysis, carried out in swDMR (https://code.google.com/p/swdmr/). The significance of the observed DMRs was determined using a three sample Kruskal-Wallis test between T0, T8 and T8P. Analysis of DMR length distribution showed DMRs sizes ranging from 12 to 4994bp (Figure 6A). The sliding window approach identified 2,822 regions as being significantly differentially methylated in one of the samples compared to the other two for all mCs (Table 2, Supplementary Table 5). Overall methylation levels of DMRs decreased in all contexts (CG, CHG and CHH) as time in culture progressed (from T1 to T8) but this was followed by a recovery of DNA methylation levels after culture on *A. thaliana* (T8P) (Figure

6b). However, it is worth noting that T8 showed a larger number of outlier DMRs (greater than two standard deviations away from the mean) that exhibited significantly higher levels of methylation than the average (Figure 6B).

When studied individually, changes in methylation levels within DMRs between samples presented two main pattern types (Table 2, Supplementary Table 5): **1.** 57.3% of the detected DMRs showed a recovery pattern inoculation on *A. thaliana* such that there was no difference between T1 and T8P samples but methylation levels diverged significantly in T8 (T1=T8P<> T8 (FDR< 0.01))). **2.** The remaining DMRs showed a non-recovery pattern (i.e., T1<> T8P (FDR< 0.01)). Two subtypes where found for DMRs showing a DNA methylation recovery pattern: **1.** DMRs showing an increase in methylation with time in culture (T1=T8P <T8 (26.82%) (defined as Type 0 hereafter) and **2.** DMRs showing a decrease in methylation level with time in culture (T1=T8P > T8 (30.47%)) (Type 2). Equally, non-recovery DMRs can be divided into two categories: **1.** DMRs showing a decrease in methylation level with time in culture and no change in methylation level following inoculation on *A. thaliana* (T0>T7=T7P (16.02%)) (Type 1a) and **2.** DMRs not showing changes in methylation level during culture but an increase in methylation level after inoculation on *A. thaliana* (T0=T7<T7P (26.68%)) (Type 1b). Curiously, no DMRs were observed to show a progressive increase in methylation level with time in culture and no change in methylation level after inoculation on *A. thaliana* (T1<T8=T8P).

The vast majority (84.5%) of detected DMRs overlapped with 3,055 genic regions in the *B. cinerea* genome (Table 3) while 438 (15.5%) mapped to intergenic regions. Almost all of the genes implicated (98%) included DMRs within the gene body itself, with a majority (53.9%) also overlapping with the promoter region (Table 3, Supplementary Table 6). The same analyses were carried out to detect DMRs for CG, CHG and CHH contexts, identifying 70,

82 and 1,248 DMRs respectively for each context (Table 3, Supplementary Table 5). Of these, 91.4% (CG), 89.0% (CHG) and 85.2% (CHH) overlapped with 68, 84 and 1,339 genes respectively (Table 3, Supplementary Table 6).

Finally, we conducted a search for DMRs overlapping with 1,577 *B. cinerea* genes with known targeted functions that was carried out in the resequencing section above. Of these, 478 genes (30.3%) overlapped with one or more detected DMRs (See Table 1 and Supplementary Table 7 for a comprehensive list of genes overlapping with DMRs).

Discussion

Culture induced changes in *B. cinerea* MSAP profiles and in virulence are simultaneous and reversible.

In accordance with previous reports (6–9), we found that virulence of *B. cinerea* cultures significantly decreases with culture age, and that virulence levels recover after one passage on *A. thaliana* (5). Concurrent with these changes, we observed that MSAP profiles showed a similar progressive increase in deviation from the starter culture profiles. This observed accumulation of somaclonal variation as culture progressed, showed a positive linear correlation with the observed changes in virulence. This correlation is consistent with previous reports of accumulative genetic/methylome change for other species when similarly exposed to prolonged periods of culture (15,29). Our observations also accord with the high levels of somaclonal variability arising during *in vitro* growth of phytopathogenic fungi, which seemingly depresses the level of virulence of the culture isolates (30). Whilst the source of the increased variation during protracted culture could have a genetic or epigenetic cause (both mutation and methylation perturb MSAP profiles), reversal of virulence

289 phenotype after a single passage of the cultured fungus on *A. thaliana* (T8P) strongly implies
290 that a plastic, epigenetic mechanism drives the observed change in virulence. This is most
291 easily explained if culture alters the methylation status of the genome and this in turn perturbs
292 virulence. For this hypothesis to hold, it is important to establish a link between changes in
293 the methylome on genes known to be implicated in virulence. This requires a more precise
294 approach to describing the global changes in methylome patterning and mutation.

295

296 **Sequence variants do not explain loss of virulence during protracted culture of *B.***
297 ***cinerea***

298 Whole genome resequencing of six DNA samples taken at two time points (one month and
299 eight months) was carried out to monitor for mutational change during the extended period of
300 *B.* cinerea culture. This yielded a total of 2,331 sequence variants of which 454 mutations
301 occurred within genes, of which only 198 were non-synonymous mutations (193 causing
302 missense variations and five causing premature stop codons (non-sense mutations). For genes
303 with unknown function, it is difficult to implicate these changes as being involved in the loss
304 of virulence observed during culture. We therefore screened specifically for the appearance
305 of genetic variants among 1,577 *B. cinerea* genes with known function of which only 4.3%
306 showed variants. Of these, just eight genes (0.5% of the total) included sequence variants that
307 were not silent mutations, or led to a conservative missense codon or a synonymous codon.
308 Of the 1184 genes known to be associated to virulence, just six (0.5%) included a sequence
309 variant that could conceivably affect the virulence phenotype. All six genes were plant cell
310 wall disassembly genes (CAZyme genes (31)). The low level of detected genetic variants and
311 specially the lack of variants on virulence *sensu stricto* genes induced by protracted *in vitro*
312 culture again supports that genetic mutation is not the primary cause of the erosion of

313 virulence during in vitro culture of *B. cinerea* a finding reported previously for other species
314 (25).

315

316 **_In vitro_ culture affects whole-genome methylation patterns in *B. cinerea***

317 Taken collectively, our results suggest that changes in DNA methylation at a genome level
318 are more likely than mutation to be causally linked to the observed loss of virulence during *in*
319 *vitro* culture. We sought to establish a more direct link between methylome changes and gene
320 activity by sequencing of the methylomes of nine samples from three culture time points (T1,
321 T8 and T8P). All genomes presented similarly low levels of DNA methylation (0.6%) as
322 reported for other fungal species (21). DNA methylation was not evenly distributed across
323 contigs but clustered into certain regions following a mosaic pattern (32), with higher levels
324 of methylation in regions with lower abundance of genes. Such clustering patterns have been
325 previously observed in pathogenic fungi linked to transposable elements rich and gene poor
326 regions (19), and have been shown to be dynamic following fungal development (19). The
327 observed clustering patterns were similar in all analysed culture time points suggesting that
328 the methylation changes detected here are not associated to progression in development
329 occurred during culture. However, global methylation levels varied with sequence context
330 (with CHH > CG > CHG) and time in culture. In brief, global methylation levels on CGs and
331 CHGs increased significantly between 1 (T1) and 8 (T8) months in culture. In both sequence
332 contexts, following inoculation on *A. thaliana*, T8P cultures had lost some of the methylation
333 accumulated during culture and were no longer significantly different to the virgin
334 inoculums. This observed change in methylation levels supports MSAP results that showed
335 an increase of methylome variation with time in culture that was only partially recovered n
336 T8P cultures.

Previous genome-wide studies have shown that gene methylation in the monophyletic Ascomycota phylum varies greatly. For example, in *Neurospora crassa* DNA methylation is not found in gene bodies. However gene body methylation has been reported in other species such as, *Candida albicans*, *Uncinocarpus reesii* and *Magnaporthe oryza* (16,19,21) while promoter methylation has only been reported in *M. oryza* (19). Analysis of the effect of methylation distribution and density on gene expression has shown that gene body methylation has positive effects on gene expression (19,21) while promoter methylation has a negative effect (19). Our analysis of methylation distribution in *B. cinerea* genes showed an increase in methylation approximately 800bp upstream of the TSS followed by a sharp decrease at the TSS as shown by Jeon et al (2015) in *M. oryza* mycelia. Our results showed a second increase in methylation density after the TSS indicating that at least some *B. cinerea* genes contain gene body methylation.

Comparative analysis between culture time points showed that when all *B. cinerea* genes were analysed collectively there were no changes in DNA methylation with time in culture (T1=T8). However, while DNA methylation on house-keeping remained stable between culture time points, CAZyme genes showed an increase in promoter methylation with time in culture (i.e. T1<T8). Moreover, CAZyme genes showed a recovery of the original methylation levels after a single passage on *A. thaliana* (i.e. T1=T8P<T8). Conversely, all *B. cinerea* genes analysed collectively showed an increase in methylation, similar to that observed at a whole genome scale (T8<T8P). Global methylation levels on the CAZyme gene in promoter showed a negative correlation with virulence levels. This observed increase in promoter methylation on T8 samples seems to be due to an increase on the CHG and CG contexts. Conversely, global methylation levels on the CAZyme gene bodies showed a

362 positive correlation with virulence levels (T1=T8P>T8) that seem to be due to changes on the
363 CHH context. CAZyme genes encode proteins that breakdown, biosynthesise and modify
364 plant cell wall components and are highly expressed during plant invasion in *B. cinerea*
365 (28,31). This gene family, should therefore, be readily accessible to the transcriptional
366 machinery in the virulent form of pathogenic fungi. Interestingly, our results show a
367 correlation between virulence levels in T1, T8 and T8P samples and a methylation features in
368 CAZyme genes that have positive effects on gene expression, i.e. high gene-body
369 methylation (19,21) and low promoter methylation (19) in high virulence cultures (T1 and
370 T8P) and the opposite in the low virulence culture (T8).

371

372 **Culture induced differentially methylated regions are reversible and mirror changes in**
373 **virulence**

374 To determine the significance of the observed changes in DNA methylation between culture
375 time points we performed an analysis of regional differential methylation identifying 2,822
376 significant DMRs in one time point compared to the other two for all mCs. Globally, DMRs
377 show a decrease in methylation level between T1 to T8 in all contexts (CG, CHG and CHH),
378 followed by a recovery of DNA methylation levels after culture on *A. thaliana* (T8P). This
379 seem to contradict the observed changes in global DNA methylation levels which showed an
380 increasing trend (T1 < T8 < T8P). However, T8 showed a larger number of outlier DMRs
381 showing levels of methylation significantly higher than the average, suggesting that not all
382 predicted DMRs followed the same pattern of demethylation followed by re-methylation.
383 Furthermore, similar differences between global and local DNA methylation levels have been
384 reported previously in different organisms (19,33). Interestingly, regional changes in DNA
385 methylation have been previously associated to the developmental potency of fungal cells
386 (19). In their work, Jeon et al (2015) showed how fungal totipotent cells (mycelia) present

387 higher global methylation levels while cells determined to host penetration (appresoria)
388 present a higher number of genes with methylated cytosines but lower global levels of DNA
389 methylation. More pertinently, 68.3% of the culture induced DNA methylation changes (i.e.
390 Type 0, 2 and 1a, which accounts for 57.3% of the total detected DMRs) showed a recovery
391 pattern after a single round of inoculation onto *A. thaliana*. This suggests that a majority of
392 the DNA methylation changes accumulated during *in vitro* culture are reset to their original
393 state after a single passage on the host. Interestingly, 26.7% of the observed changes (Type
394 1b) were not induced by *in vitro* culture but by the host. This highlights, as shown before in
395 other pathogens (2,34,35), the importance of epigenetic mechanisms in host/pathogen
396 interactions, and the potential implication of dynamic DNA methylation as regulator of
397 phenotypic plasticity in response to nutrient availability and interaction with the host (36).

398

399 Of the total detected DMRs for all mCs 84.5% overlapped with one or more genes suggesting
400 that the great majority of *in vitro* culture induced DNA methylation changes occur in genic
401 regions. This overlap of individual DMRs with one than more gene is probably partially due
402 to the small average size of intergenic regions (778 to 958bp) and genes (744 to 804 bp) in *B.*
403 *cinerea* (26). Analysis of DMRs overlapping with 1,577 genes with known function revealed
404 that 30.3% of the total overlapped with DMRs. Ten gene functional groups (house-keeping,
405 apoptosis, conidiation, mating and fruit body development, secondary metabolism, signaling,
406 sclerotium formation, appresorium formation, virulence and CAZYme genes) were screened
407 for overlapping DMRs. House-keeping genes did not overlap with any DMRs while genes
408 associated to apoptosis and conidiation showed the higher percentage of overlapping with
409 DMRs (40.0 And 37.5% respectively). Remarkably, both biological processes have been
410 previously shown to be affected by DNA methylation (19,37,38). Moreover, 98% of these
411 DMRs overlapped, at least partially, with gene bodies while 2.4% and 15.6% overlapped only

412 with promoters or gene bodies respectively. Taken collectively, this indicates that *B. cinerea*
413 genes in general and gene bodies in particular are prone to environmentally-induced change
414 to their methylation status. When DMRs were defined using each DNA methylation context
415 independently (i.e. CG, CHG and CHH), the large majority (89.1% of all DMRs and 89.9%
416 of those overlapping with genes) were linked to changes on the CHH context, implying that
417 DMRs in this context are the reason for the observed changes in detected CAZyme gene body
418 methylation associated to higher levels of virulence.

419

420 **Conclusion**

421 In this study, we present, to our knowledge, the first proof that global and local changes in
422 DNA methylation are linked to virulence changes during *in vitro* culture. Furthermore, here
423 we present the first single base resolution DNA methylome for the plant pathogen *B. cinerea*.
424 Our results suggest that protracted culture of *B. cinerea* induces a hypermethylated, low
425 pathogenic form adapted to the absence of the host or the abundance of nutrients in the
426 culture media. It is tempting to speculate that the observed change in global and local levels
427 of DNA methylation during *in vitro* culture could be part of a mechanism that confers
428 plasticity to the *B. cinerea* genome to adapt to different environments. Butt et al (2006)
429 proposed that *in vitro* culture induced loss of virulence could be the reflexion of an adaptive
430 trait selected to promote energy efficiency, i.e. by turning off virulence genes in the absence
431 of the host or in environments rich in freely available nutrients. The authors also proposed
432 that this trait could become maladaptive since it restricts the pathogen to a saprophytic mode
433 (5). Environmentally induced epigenetic adaptive changes have been predicted to have the
434 potential to induce evolutionary traps leading to maladaptation (39,40). However, in this case
435 the complete reversibility of the reduced virulence phenotype induced by protracted culture
436 suggests that this might not be the case.

437

438 In our view, the availability of an increasingly large number of sequenced genomes and
439 methylomes from pathogenic fungi, together with our ability to decipher the associations
440 between changes in DNA methylation and virulence, will stimulate our understanding of the
441 mechanisms involved in the control of pathogenicity on these species. Moreover, the analysis
442 of DMRs could potentially be used to predict gene function in non-model fungal species or
443 even to predict pathogenicity in wild strains. More importantly, if the epigenetic regulation of
444 the transition between the virulent and non-virulent states that we propose here applies
445 broadly to other pathogenic fungi, our findings will open the door to a new type of non-lethal
446 fungicide aimed at maintaining pathogenic fungi as saprotrophic that by its nature would
447 reduce the appearance of resistant strains.

448

449 **Materials and Methods**

450 ***Botrytis cinerea* culture and inoculation**

451 7 *Botrytis cinerea* cultures (IMI169558 isolate (41)) were initiated from a single frozen
452 inoculum and cultured and harvested for 32 weeks as stated in Johnson et al (42). After 4
453 weeks in culture (T0) the initial culture was subcultured to 7 plates containing fresh medium.
454 Mycelium from each plate was subsequently subcultured every 4 weeks (1 month hereafter)
455 to fresh medium. A mycelium sample was taken for DNA extraction from all replicates and
456 conidia harvested for virulence analysis (42) from five replicates at every subculture. For
457 assessments of infection phenotypes, single leaves from five *Arabidopsis thaliana* Col 0
458 plants (leaf stage 7 or 8 as defined by (43)) were inoculated with 5 µl of spore suspension
459 collected at each subculture time (T0-T8), pipetted onto the adaxial surface of the leaf.
460 Controls were inoculated with PDB. Finally, after the T8 challenge, *B. cinerea* was isolated

461 from the infected areas, cultured and immediately used to challenge *A. thaliana* plants to test
462 virulence recovery (Figure S2) (T8P). Plants remained under Stewart Micropropagators to
463 sustain a relative humidity of 50–80% and lightly watered every 24 h.

464

465 **Plant material**

466 *A. thaliana* Col-0 seeds were obtained from the Nottingham Arabidopsis Stock Centre
467 (NASC). Plants were cultivated as stated in (44) in Levington Universal compost in trays
468 with 24-compartment inserts. Plants were maintained in Conviron (Controlled Environments
469 Ltd) growth rooms at 24 C with a light intensity of 110 µmol m-2 s-2 and an 8 h photoperiod
470 for 4 weeks. For ease of treatment, plants were transferred to Polysec growth rooms (Polysec
471 Cold Rooms Ltd, UK; http://www.polysec.co.uk/), maintained at the same conditions.

472

473 **DNA isolation**

474 126 *B. cinerea* genomic DNA (gDNA) extractions were performed (from 2 replicates of each
475 of the 7 plates at *in vitro* time point (T1-T8) and from of the last time point culture
476 transplanted onto to *A. thaliana* (T8P)) using the DNeasy 96 Plant Kit (Qiagen, Valencia,
477 CA) and the Mixer Mill MM 300 (Retsch, Germany). Isolated DNA was diluted in nanopure
478 water to produce working stocks of 10 ng.µl^{-1}. DNA from *B. cinerea* inoculated *A. thaliana*
479 was extracted from five leaf samples at each time point of using a DNeasy Mini Kit (Qiagen,
480 Valencia, CA) and the Mixer Mill MM 300 (Retsch, Germany). DNA samples were diluted
481 to 1 ng.µl^{-1} nanopure water.

482

483 **Scoring *B. cinerea* lesion phenotypes**

Disease lesions were assessed 3 days post inoculation. A weighted scoring method was used to categorize *B. cinerea* lesion phenotypes (45). High virulence symptoms (water-soaking, chlorosis, and spreading necrosis) were conferred a range of positive scores and the resistant symptoms (necrosis limited to inoculation site) were given negative scores (Figure 1A). A weighted score was produced arithmetically from the lesion scores of replicates. Inoculated *A. thaliana* leaves at T0, T8 and T8P were collected 3 days after inoculation for estimation of *in planta* fungal development by quantitative PCR **(**Figure S2**)**.

Estimation of *in planta* fungal growth by quantitative PCR

Quantitative real-time PCR (qPCR) reactions (25 µl) were prepared by mixing 10 µl DNA solution with 12.5 µl of SYBR™ Green Mastermix (Applied Biosystems, UK) and primers (to a final concentration of 300 nM). Primer for Arabidopsis to generated a 131 bp amplicon of the Shaggy-kinase-like gene (ASK) ((iASK1: CTTATCGGATTTCTCTATGTTTGGC; iASK2: GAGCTCCTGTTTATTTAACTTGTACATACC). Primers for *B. cinerea.* (CG11: AGCCTTATGTCCCTTCCCTTG; CG12: GAAGAGAAATGGAAAATGGTGAG to generated a Cutinase A gene 58 bp amplicon (24). qPCRs were carried out using a Bio-Rad ABI7300 thermocycler amplifying using the following conditions: 15 min at 95 °C followed by 50 cycles of 95 °C for 15 s, 58 °C for 30 s and 72 °C for 1 min. This was followed by a dissociation (melting curve), according to the software procedure. Serial dilutions of pure genomic DNA from each species were used to trace a calibration curve, which was used to quantify plant and fungal DNA in each sample. Results were expressed as the CG11/iASK ratio of mock-inoculated samples.

MSAP procedure

We used a modification of the MSAP methods (46,47) to reveal global variability in CG methylation patterns between *B. cinerea* samples. A total of 14 samples per time point (T1 to T7P) were analysed (2 replicated DNA extractions per culture plate). For each individual sample, 50ng of DNA were digested and ligated for 2 h at 37°C using 5U of *Eco*RI and 1U of *Msp*I or *Hpa*II (New England Biolabs), 0.45 µM *Eco*RI adaptor, 4.5 µM *Hpa*II adaptor (Supplementary Table 8 for oligonucleotide sequences) and 1U of T4 DNA ligase (Sigma) in 11 µl total volume of 1X T4 DNA ligase buffer (Sigma), 1µl of 0.5M NaCl, supplemented with 0.5 µl at 1mg/ml of BSA. Enzymes were then inactivated by heating to 75°C for 15 min. Following restriction and adaptor ligation there followed two successive rounds of PCR amplification. For preselective amplification, 0.3 µl of the restriction/ligation products described above were incubated in 12.5 µl volumes containing 1X Biomix (Bioline, London, UK) with 0.05 µl of Preamp EcoRI primer and 0.25 µl Preamp HpaII/MspI (both primers at 10 uM) (Supplementary Table 8) supplemented with 0.1 µl at 1mg/ml of BSA. PCR conditions were 2 min at 72°C followed by 30 cycles of 94°C for 30 s, 56°C for 30 s and 72°C for 2 min with a final extension step of 10 min at 72°C. Selective PCR reactions were performed using 0.3 µl of preselective PCR reaction product and the same reagents as the preselective reactions but using FAM labelled selective primers (E2/H1; Supplementary Table 8). Cycling conditions for selective PCR were as follows: 94°C for 2 min, 13 cycles of 94°C for 30 s, 65°C (decreasing by 0.7°C each cycle) for 30 s, and 72°C for 2 min, followed by 24 cycles of 94°C for 30 s, 56°C for 30 s, and 72°C for 2min, ending with 72°C for 10 min. Fluorescently labelled MSAP products were diluted 1:10 in nanopure sterile water and 1 µl was combined with 1 µl of ROX/HiDi mix (50 µl ROX plus 1 ml of HiDiformamide, Applied Biosystems, USA). Samples were heat-denatured at 95°C for 3–5 min and snap-cooled on ice for 2 min. Samples were fractionated on an ABI PRISM 3100 at 3 kV for 22 s and at 15 kV for 45 min.

533

534 **Analysis of genetic/epigenetic variability during time in culture using MSAP**

535 MSAP profiles were visualized using GeneMapper Software v4 (Applied Biosystems, Foster
536 City, CA). A qualitative analysis was carried out in which epiloci were scored as ‘‘present’’
537 (1) or ‘‘absent’’ (0) to form a presence/absence binary matrix. The selection of MSAP
538 fragments was limited to allelic sizes between 80 and 585bp to reduce the potential impact of
539 size homoplasy (48). Samples were grouped according to the time in culture when they were
540 collected (1, 2, 3, 4, 5, 6, 7, 8 months and 8 months and inoculation onto *A. thaliana* called
541 T1, T2, T3, T4, T5, T6, T7 and T7P hereafter). MSAP profile polymorphisms between DNA
542 samples from different culture time points were considered as *in vitro* culture induced
543 methylation differences.

544

545 Epigenetic similarity between tested samples based on profiles obtained from primer
546 combination E2/H1 and both enzymes (*Hpa*II and *Msp*I) was first visualized using Principal
547 Coordinate Analysis (PCoA) (49) using GenAlex (v.6.4) (50). We then used Analysis of
548 Molecular Variance (AMOVA) (51) to evaluate the structure and degree of epigenetic
549 diversity induced by different times in culture. Pairwise PhiPT (52) comparisons between
550 samples restricted with *Hpa*II or *Msp*I from each time point and the samples after the first
551 passage (2 months in culture, T1) were used to infer their overall level of divergence in DNA
552 methylation with time in culture (i.e., the lower the PhiPT value between samples T1
553 restricted using *Hpa*II or *Msp*I the smaller the differentiation induced by culture and the same
554 samples). AMOVA was subsequently calculated using GenAlex (v.6.5) to test the
555 significance of PhiPT between populations (52), with the probability of non-differentiation
556 (PhiPT=0) being estimated over 9,999 random permutations.

Mantle test analysis was used to estimate the correlation between the calculated pairwise genetic/epigenetic distances and the difference in virulence between culture time points. The level of significance was assigned estimated over 9,999 random permutations tests, as implemented in Genalex v6.5.

Methylation analysis by bisulphite sequencing

DNA from 9 biological replicates from culture of two different ages (1, 8 months) and from 9 replicates of tissue recovered from samples culture for eight months and the inoculated onto an *A. thaliana* plant were randomly selected for sequencing. Biological replicates were used to generate 3 pooled samples per culture age. Bisulphite treatment was performed independently from 50ng of genomic DNA of each pooled sample using the EZ DNA methylation-Gold™ Kit (Zymo Research) according to the manufacturers' instructions adjusting the final column purification elution volume to 10 µl. Following Bisulphite treatment, recovered DNA from each pool was used to estimate yield using a NanoDrop 100 spectrophotometer with the RNA setting. The remaining bisulphite treated sample were then used to create a sequencing library using the EpiGnome™ Methyl-Seq Kit (Epicentre) according to manufacturer's instructions and using EpiGnome™ Index PCR Primers (4-12).

In order to provide a reference draft sequence for the alignment of the bisulphite treated DNA and to detect any culture induced genetic variability, 10 ng of native (non-bisulphite treated) DNA extracted from 3 independent cultures from two time points (1 month (T1) and 8 month (T8)) were pooled by time point, sequenced and compared to the B. *cinerea* B05.10 genome sequence. Sequencing libraries were prepared using the EpiGnome™ Methyl-Seq Kit

(Epicentre) according to manufacturer's instructions. Native DNA libraries were uniquely indexed using EpiGnome™ Index PCR Primers (Epicentre) (1-3).

Library yield was determined by Qubit dsDNA High Sensitivity Assay Kit. Agilent 2100 Bioanalyzer High-Sensitivity DNA Chip was used to assess library quality and determine average insert size. Libraries were then pooled and sequenced on Illumina HiSeq 2000 (Illumina Inc., San Diego, CA) using 100bp paired end V3 chemistry by QBI Centre for Brain Genomics.

Sequence analysis and differential methylation analysis

Obtained sequencing reads were trimmed to remove adaptors using *TrimGalore*! (http://www.bioinformatics.babraham.ac.uk/projects/trim_galore) and *Cutadapt* (53). Whole genome re-sequencing reads were aligned to the published genome from *B. cinerea* B05.10 (Broad Institute's *B. cinerea* Sequencing Project; https://www.broadinstitute.org/scientific-community/science/projects/fungal-genome-initiative/botrytis-cinerea-genome-project) using *bowtie2* (54) and variants were called using *freebayes* (55). Variant categories were analysed using *CooVar* (56), *bedtools* (57) and custom scripts. Bisulfite treated libraries were mapped using Bismark (Krueger and Andrews, 2011) and bowtie2, duplicates removed and methylation calls were extracted using samtools (58) and in-house scripts. Bisulfite sequencing efficiency was calculated by aligning reads to the B. *cinerea* mitochondrial genome scaffold (B05.10) and identifying non-bisulfite converted bases. Differentially methylated regions were called using a sliding window approach described in swDMR (https://code.google.com/p/swdmr/) using and Kruskal-Wallis (3 sample) statistical tests.

Author contributions:

J.B. did sequence data analysis and helped drafting the manuscript. A.S. cultured the *Botrytis* samples and performed the virulence analysis. A.A. undertook the estimations of *in planta* fungal develop using qPCR. M.W. and L.A.J.M. helped to conceive the study and drafting the manuscript. C.M.R.L. conceived the study, carried out all nucleic acid extractions, performed and analysed the MSAPs, performed and assisted analysing the native and bisulfite treated DNA sequencing and wrote the manuscript. All authors have read and approved the final manuscript.

Bibliography

1. Fournier E, Gladieux P, Giraud T. The “Dr Jekyll and Mr Hyde fungus”: noble rot versus gray mold symptoms of Botrytis cinerea on grapes. Evol Appl. 2013 Sep;6(6):960–969.

2. Weiberg A, Wang M, Lin FM, Zhao H, Zhang Z, Kaloshian I, et al. Fungal small RNAs suppress plant immunity by hijacking host RNA interference pathways. Science. 2013 Oct 4;342(6154):118–123.

3. Martinez F, Dubos B, Fermaud M. The Role of Saprotrophy and Virulence in the Population Dynamics of Botrytis cinerea in Vineyards. Phytopathology. 2005 Jun;95(6):692–700.

4. Pathirana R, Cheah LH, Carimi F, Carra A. Low temperature stored in cryobank® maintains pathogenicity in grapevine. cryoletters. 2009; 30(1):84.

5. Butt T, Wang C, Shah F, Hall R. DEGENERATION OF ENTOMOGENOUS FUNGI. In: EILENBERG J, HOKKANEN H, editors. An Ecological and Societal Approach to Biological Control. Dordrecht: Springer Netherlands; 2006. p. 213–226.

6. Castro M, Kramer K, Valdivia L, Ortiz S, Castillo A. A double-stranded RNA mycovirus confers hypovirulence-associated traits to Botrytis cinerea. FEMS Microbiol Lett. 2003 Nov 7;228(1):87–91.

7. Chu YM, Jeon JJ, Yea SJ, Kim YH, Yun SH, Lee YW, et al. Double-stranded RNA mycovirus from Fusarium graminearum. Appl Environ Microbiol. 2002 May;68(5):2529–2534.

8. Hatta R, Ito K, Hosaki Y, Tanaka T, Tanaka A, Yamamoto M, et al. A conditionally dispensable chromosome controls host-specific pathogenicity in the fungal plant pathogen Alternaria alternata. Genetics. 2002 May;161(1):59–70.

9. Akamatsu H, Taga M, Kodama M, Johnson R, Otani H, Kohmoto K. Molecular karyotypes for Alternaria plant pathogens known to produce host-specific toxins. Curr Genet. 1999 Jul;35(6):647–656.

10. Kelly SA, Panhuis TM, Stoehr AM. Phenotypic plasticity: molecular mechanisms and adaptive significance. Compr Physiol. 2012 Apr;2(2):1417–1439.

11. WADDINGTON C. Canalization of Development and the Inheritance of Acquired Characters. Nature. 1942 Nov 14;150(3811):563–565.

12. Tricker PJ, Gibbings JG, Rodríguez López CM, Hadley P, Wilkinson MJ. Low relative humidity triggers RNA-directed de novo DNA methylation and suppression of genes controlling stomatal development. J Exp Bot. 2012 Jun;63(10):3799–3813.

13. Geyer KK, Rodríguez López CM, Chalmers IW, Munshi SE, Truscott M, Heald J, et al. Cytosine methylation regulates oviposition in the pathogenic blood fluke Schistosoma mansoni. Nat Commun. 2011 Aug 9;2:424.

14. Bird A. Perceptions of epigenetics. Nature. 2007 May 24;447(7143):396–398.

15. Rodríguez López CM, Wilkinson MJ. Epi-fingerprinting and epi-interventions for improved crop production and food quality. Front Plant Sci. 2015 Jun 5;6:397.

16. Su Z, Han L, Zhao Z. Conservation and divergence of DNA methylation in eukaryotes: new insights from single base-resolution DNA methylomes. Epigenetics. 2011 Feb 1;6(2):134–140.

17. He XJ, Chen T, Zhu JK. Regulation and function of DNA methylation in plants and animals. Cell Res. 2011 Mar;21(3):442–465.

18. Jupe ER, Magill JM, Magill CW. Stage-specific DNA methylation in a fungal plant pathogen. J Bacteriol. 1986 Feb;165(2):420–423.

19. Jeon J, Choi J, Lee GW, Park SY, Huh A, Dean RA, et al. Genome-wide profiling of DNA methylation provides insights into epigenetic regulation of fungal development in a plant pathogenic fungus, Magnaporthe oryzae. Sci Rep. 2015 Feb 24;5:8567.

20. Armaleo D, Miao V. Symbiosis and DNA methylation in the Cladonia lichen fungus. Symbiosis. 1999;26(2):143 – 163.

21. Zemach A, McDaniel IE, Silva P, Zilberman D. Genome-wide evolutionary analysis of eukaryotic DNA methylation. Science. 2010 May 14;328(5980):916–919.

22. Boyko A, Kovalchuk I. Genetic and epigenetic effects of plant-pathogen interactions: an evolutionary perspective. Mol Plant. 2011 Nov;4(6):1014–1023.

669 23. Reyna-López GE, Simpson J, Ruiz-Herrera J. Differences in DNA methylation patterns
670 are detectable during the dimorphic transition of fungi by amplification of restriction
671 polymorphisms. Mol Gen Genet. 1997 Feb 27;253(6):703–710.

672 24. Gachon C, Saindrenan P. Real-time PCR monitoring of fungal development in
673 Arabidopsis thaliana infected by Alternaria brassicicola and Botrytis cinerea. Plant
674 Physiol Biochem. 2004 May;42(5):367–371.

675 25. Jeon J, Choi J, Lee GW, Dean RA, Lee YH. Experimental evolution reveals genome-
676 wide spectrum and dynamics of mutations in the rice blast fungus, Magnaporthe oryzae.
677 PLoS ONE. 2013 May 31;8(5):e65416.

678 26. Amselem J, Cuomo CA, van Kan JA, Viaud M, Benito EP, Couloux A, et al. Genomic
679 analysis of the necrotrophic fungal pathogens Sclerotinia sclerotiorum and Botrytis
680 cinerea. PLoS Genet. 2011 Aug 18;7(8):e1002230.

681 27. Choquer M, Fournier E, Kunz C, Levis C, Pradier JM, Simon A, et al. Botrytis cinerea
682 virulence factors: new insights into a necrotrophic and polyphageous pathogen. FEMS
683 Microbiol Lett. 2007 Dec;277(1):1–10.

684 28. Blanco-Ulate B, Morales-Cruz A, Amrine KC, Labavitch JM, Powell AL, Cantu D.
685 Genome-wide transcriptional profiling of Botrytis cinerea genes targeting plant cell
686 walls during infections of different hosts. Front Plant Sci. 2014 Sep 3;5:435.

687 29. Rodríguez López CM, Wetten AC, Wilkinson MJ. Progressive erosion of genetic and
688 epigenetic variation in callus-derived cocoa (Theobroma cacao) plants. New Phytol.
689 2010 Jun;186(4):856–868.

690 30. Dahmen H, Staub T, Schwinn FJ. Technique for Long-Term Preservation of
691 Phytopathogenic Fungi in Liquid Nitrogen. Phytopathology. 1983;73(2):241.

692 31. Lombard V, Golaconda Ramulu H, Drula E, Coutinho PM, Henrissat B. The
693 carbohydrate-active enzymes database (CAZy) in 2013. Nucleic Acids Res. 2014
694 Jan;42(Database issue):D490–D495.

695 32. Feng S, Cokus SJ, Zhang X, Chen PY, Bostick M, Goll MG, et al. Conservation and
696 divergence of methylation patterning in plants and animals. Proc Natl Acad Sci U S A.
697 2010 May 11;107(19):8689–8694.

698 33. Jung M, Pfeifer GP. Aging and DNA methylation. BMC Biol. 2015 Jan 31;13:7.

699 34. Gómez-Díaz E, Jordà M, Peinado MA, Rivero A. Epigenetics of host-pathogen
700 interactions: the road ahead and the road behind. PLoS Pathog. 2012 Nov
701 29;8(11):e1003007.

702 35. Cheeseman K, Weitzman JB. Host-parasite interactions: an intimate epigenetic
703 relationship. Cell Microbiol. 2015 Aug;17(8):1121–1132.

36. Mishra PK, Baum M, Carbon J. DNA methylation regulates phenotype-dependent transcriptional activity in Candida albicans. Proc Natl Acad Sci U S A. 2011 Jul 19;108(29):11965–11970.

37. Hervouet E, Cheray M, Vallette FM, Cartron PF. DNA methylation and apoptosis resistance in cancer cells. Cells. 2013 Jul 18;2(3):545–573.

38. Belden WJ, Lewis ZA, Selker EU, Loros JJ, Dunlap JC. CHD1 remodels chromatin and influences transient DNA methylation at the clock gene frequency. PLoS Genet. 2011 Jul 21;7(7):e1002166.

39. O'Dea RE, Noble DWA, Johnson SL, Hesselson D, Nakagawa S. The role of non-genetic inheritance in evolutionary rescue: epigenetic buffering, heritable bet hedging and epigenetic traps. Environmental epigenetics. 2016;2(1):dvv014.

40. Consuegra del Olmo S, Rodriguez Lopez CM. Epigenetic-induced alterations in sex-ratios in response to climate change: an epigenetic trap? BioEssays.

41. Thomma BP, Eggermont K, Tierens KF, Broekaert WF. Requirement of functional ethylene-insensitive 2 gene for efficient resistance of Arabidopsis to infection by Botrytis cinerea. Plant Physiol. 1999 Dec;121(4):1093–1102.

42. Johnson H, Lloyd A, Mur L, Smith A, Causton D. The application of MANOVA to analyse Arabidopsis thaliana metabolomic data from factorially designed experiments. Metabolomics. 2007 Nov 7;3(4):517–530.

43. Boyes DC, Zayed AM, Ascenzi R, McCaskill AJ, Hoffman NE, Davis KR, et al. Growth stage-based phenotypic analysis of Arabidopsis: a model for high throughput functional genomics in plants. Plant Cell. 2001 Jul;13(7):1499–1510.

44. Johnson H, Broadhurst D, Goodacre R, Smith A. Metabolic fingerprinting of salt-stressed tomatoes. Phytochemistry. 2003 Mar;62(6):919–928.

45. Lloyd AJ, William Allwood J, Winder CL, Dunn WB, Heald JK, Cristescu SM, et al. Metabolomic approaches reveal that cell wall modifications play a major role in ethylene-mediated resistance against Botrytis cinerea. Plant J. 2011 Sep;67(5):852–868.

46. Róis AS, Rodríguez López CM, Cortinhas A, Erben M, Espírito-Santo D, Wilkinson MJ, et al. Epigenetic rather than genetic factors may explain phenotypic divergence between coastal populations of diploid and tetraploid Limonium spp. (Plumbaginaceae) in Portugal. BMC Plant Biol. 2013 Dec 6;13:205.

47. Rodríguez López C, Morán P, Lago F, Espiñeira M, Beckmann M, Consuegra S. Detection and quantification of tissue of origin in salmon and veal products using methylation sensitive AFLPs. Food Chem. 2012 Apr;131(4):1493–1498.

738 48. Caballero A, Quesada H, Rolán-Alvarez E. Impact of amplified fragment length
739 polymorphism size homoplasy on the estimation of population genetic diversity and the
740 detection of selective loci. Genetics. 2008 May;179(1):539–554.

741 49. Gower JC. Some Distance Properties of Latent Root and Vector Methods Used in
742 Multivariate Analysis. Biometrika. 1966 Dec; 53(3/4):325–338

743 50. Peakall R, Smouse PE. GenAlEx 6.5: genetic analysis in Excel. Population genetic
744 software for teaching and research--an update. Bioinformatics. 2012 Oct
745 1;28(19):2537–2539.

746 51. Excoffier L, Smouse PE, Quattro JM. Analysis of molecular variance inferred from
747 metric distances among DNA haplotypes: application to human mitochondrial DNA
748 restriction data. Genetics. 1992 Jun;131(2):479–491.

749 52. Michalakis Y, Excoffier L. A generic estimation of population subdivision using
750 distances between alleles with special reference for microsatellite loci. Genetics. 1996
751 Mar;142(3):1061–1064.

752 53. Martin M. Cutadapt removes adapter sequences from high-throughput sequencing
753 reads. EMBnet.journal. 2011 May 2;17(1):10.

754 54. Langmead B, Salzberg SL. Fast gapped-read alignment with Bowtie 2. Nat Methods.
755 2012 Apr;9(4):357–359.

756 55. Garrison E, Marth G. Haplotype-based variant detection from short-read sequencing.
757 2012 Jul 17; Available from: https://arxiv.org/abs/1207.3907

758 56. Vergara IA, Frech C, Chen N. CooVar: co-occurring variant analyzer. BMC Res Notes.
759 2012 Nov 1;5:615.

760 57. Quinlan AR, Hall IM. BEDTools: a flexible suite of utilities for comparing genomic
761 features. Bioinformatics. 2010 Mar 15;26(6):841–842.

762 58. Li H, Handsaker B, Wysoker A, Fennell T, Ruan J, Homer N, et al. The Sequence
763 Alignment/Map format and SAMtools. Bioinformatics. 2009 Aug 15;25(16):2078–
764 2079.

765

766

FIGUREs AND TABLES

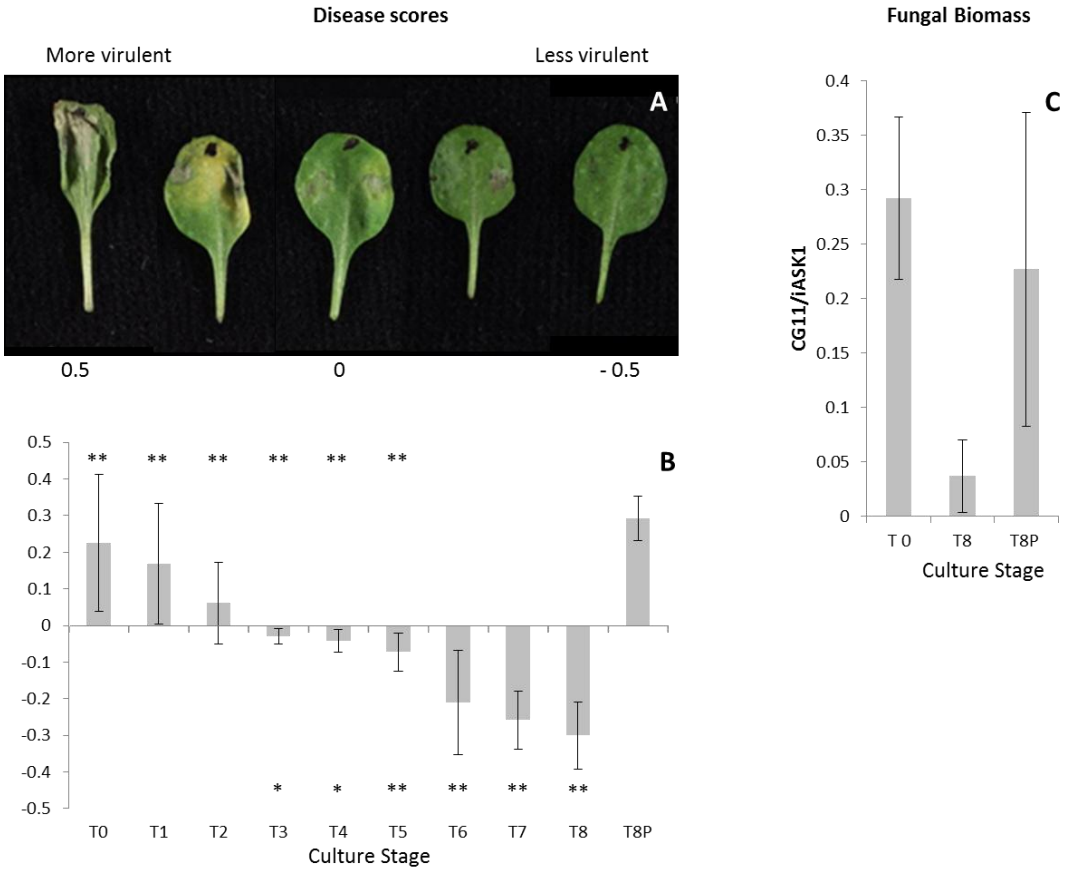

Figure 1: Estimation of *Botrytis cinerea* virulence on *Arabidopsis thaliana*. (a) Examples of *A. thaliana* Col-0 leaves drop inoculated with *B. cinerea* and presenting disease scores ranging from -0.5 (low virulence) to 0.5 (high virulence). **(b)** Estimated *B. cinerea* virulence at each time culture point. Virulence of *B. cinerea* cultures was estimated over a period of eight months in culture (T0, initial inoculum; T8, eight months in culture) and after 8 months in culture and a single passage on *A. thaliana* (T8P). A weighted scoring method was used to categorize *B. cinerea* lesion phenotypes 3 days post inoculation. Virulence symptoms (water-soaking, chlorosis, and spreading necrosis) were conferred a range of positive scores and the

781 resistant symptoms (necrosis limited to inoculation site) were given negative scores. Asterisk
782 symbols under the horizontal axis indicate significant differences (*(T-Test; P< 0.05) and **
783 (T-Test; P< 0.01)) between T0 and the time point over the asterisk. Asterisk symbols over the
784 horizontal axis indicate significant differences (** (T-Test; P< 0.01)) between T8P and the
785 time point under the asterisk. **(c)** Detection of *in planta B. cinerea* hyphal mass in *A. thaliana*
786 Col-0 by qPCR as described by Gachon and Saindrenan, 2004.

787
788

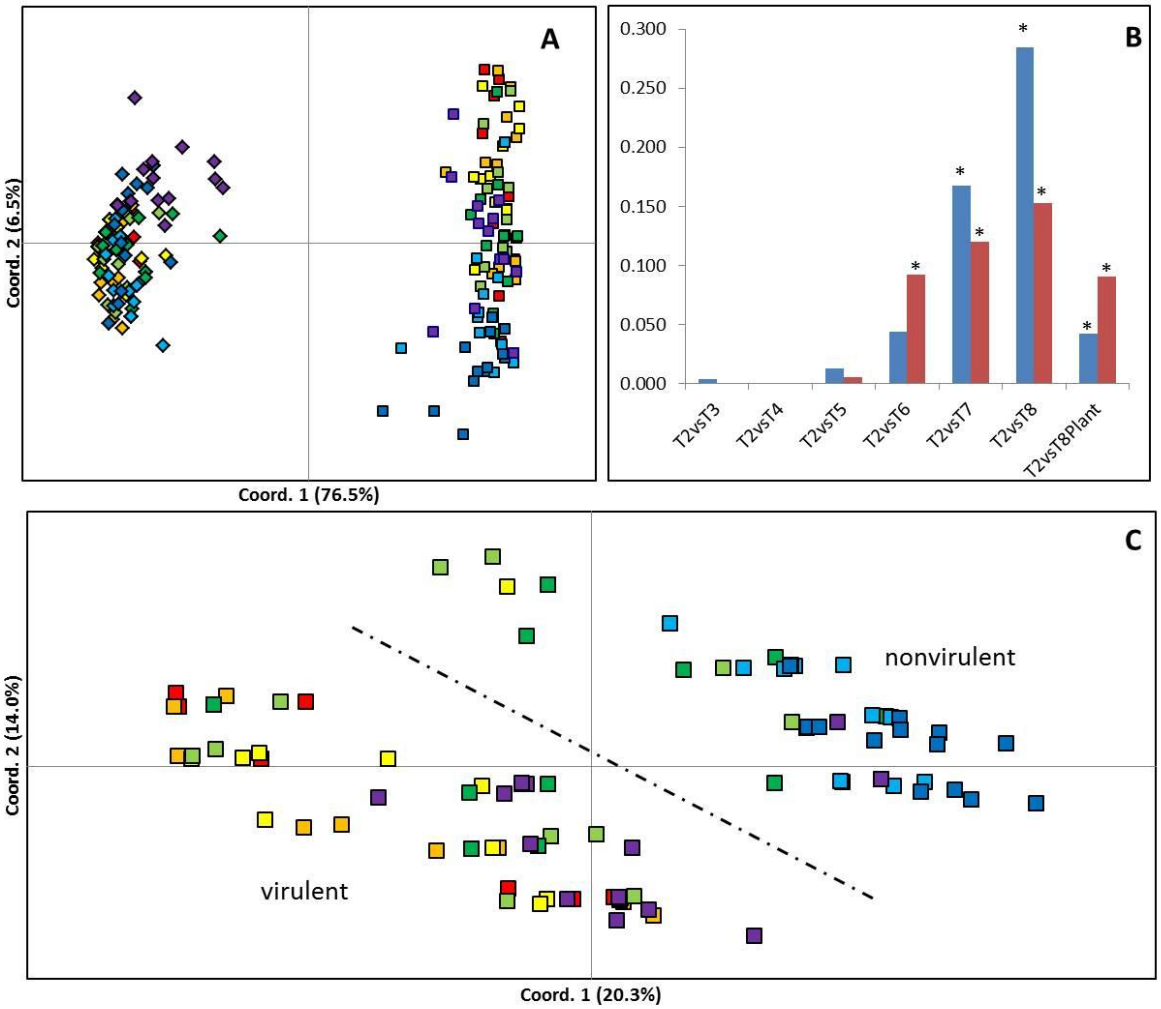

Figure 2: Effect of time in culture on genetic/epigenetic instability. (a, c) Principal coordinate diagrams based on the Euclidian analysis of methylation-sensitive amplified polymorphisms (MSAP) using enzymes *Hpa*II (squares) and *Msp*I (romboids) **(a)** and using enzyme *Hpa*II distances **(c)**. 14 replicates from each time point are represented as red (T2: 2 months in culture), orange (T3: 3 months in culture), yellow (T4: 4 months in culture), light green (T5: 5 months in culture), dark green (T6: 6 months in culture), light blue (T7: 7 months in culture), dark blue (T8: 8 months in culture), and purple (T8P: 8 months+plant). The dashed line separates samples with higher average levels of virulence from those of lower average levels of virulence. **(b)** Calculated Pairwise PhiPT (Michalakis & Excoffier, 1996) comparisons between samples restricted with *Hpa*II (Blue) or *Msp*I (Red) from each

800 time point and the samples after the second passage (2 months in culture). * Indicates
801 significantly different PhiPT values between T2 and the time point under the asterix based on
802 10,000 permutations (P = 0.05).

803
804

805

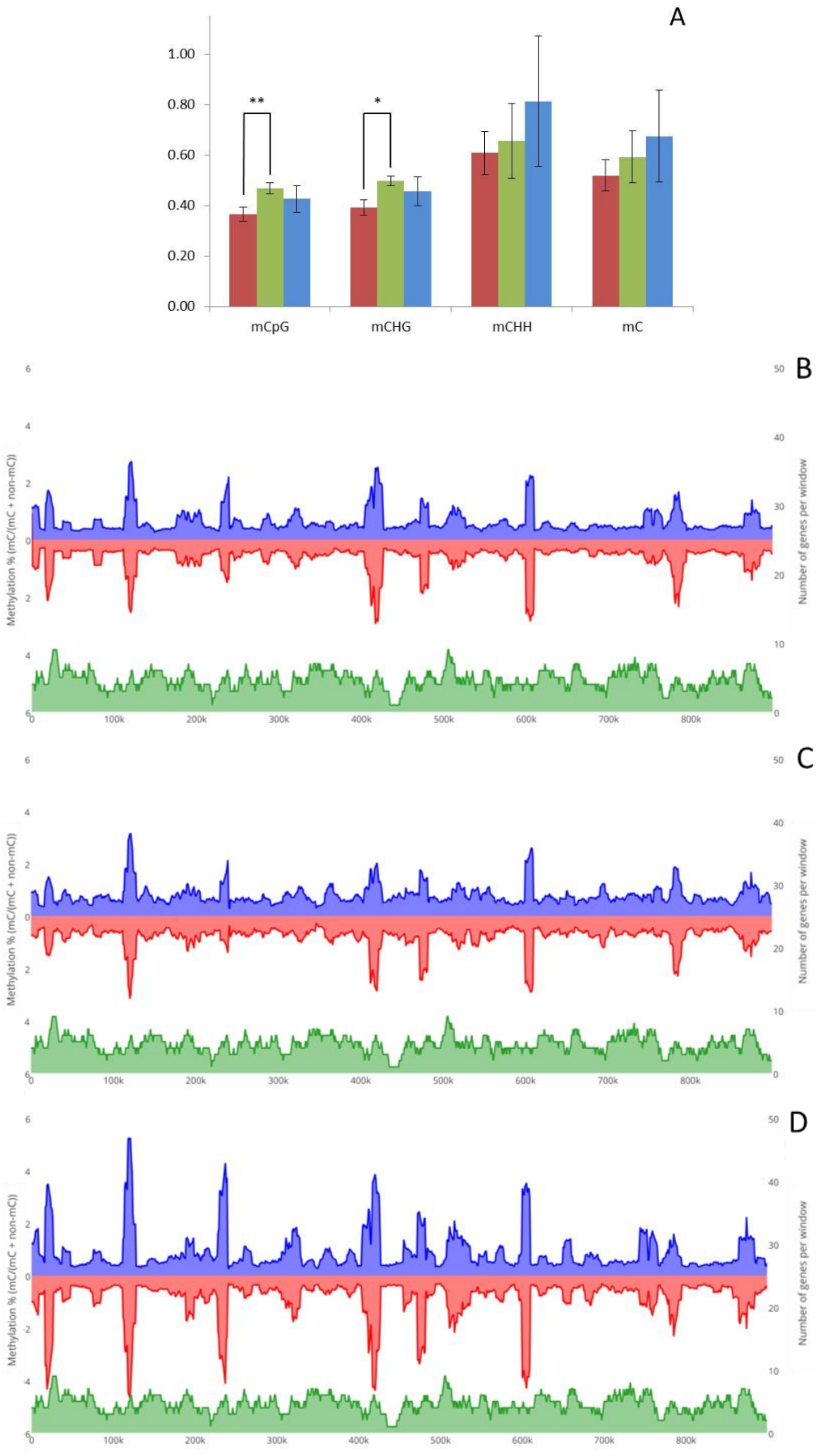

806

807 **Figure 3. Global changes on genomic distribution and levels of DNA methylation in B.**
808 **cinerea. A)** Global average proportions of mCs (number of mCs/total Cs) at each time point
809 (T1, red; T8, green and T8P, blue). **B-D)** Methylcytosines (mCs) density from each strand
810 (blue, positive and red, negative strand) across supercontig 1.1 at each time point (**B**=T1;
811 **C**=T8 and **D**=T8P) was calculated and plotted as the proportion of methylated cytosines
812 (mCs/total Cs) in each 10kb window.

813

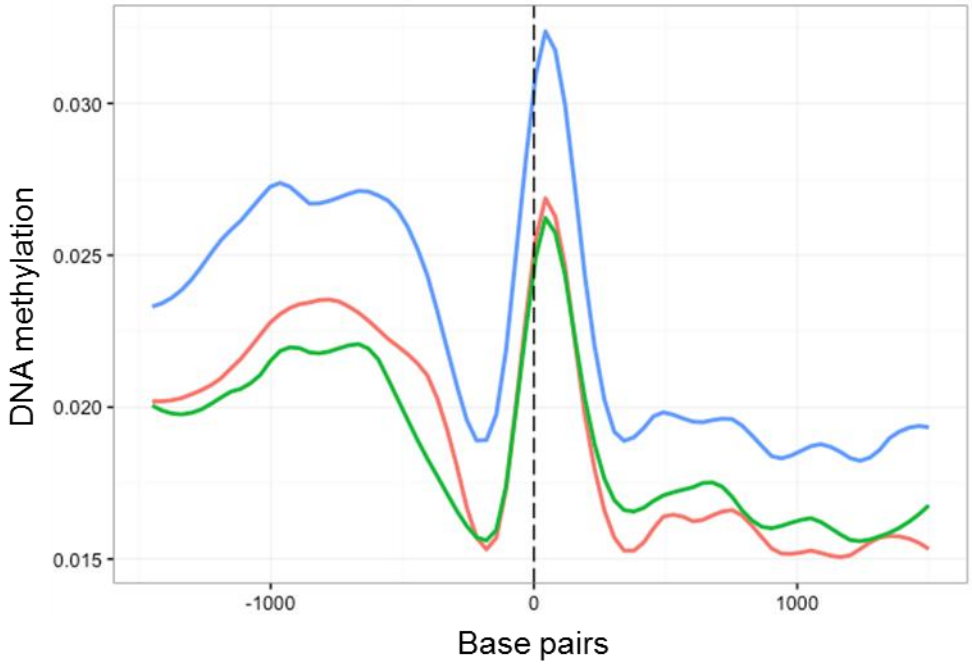

814

815 **Figure 4: Methylation density across transcription start sites (TSS) regions of all *B.***
816 ***cinerea* selected genes.** Methylation level (Vertical axis) at each time point (T1, red; T8,
817 green and T8P, blue) was identified as the proportion of methylated cytosines against all
818 cytosines in 30bp windows 1.5kb before and after the transcription start site.

819

820

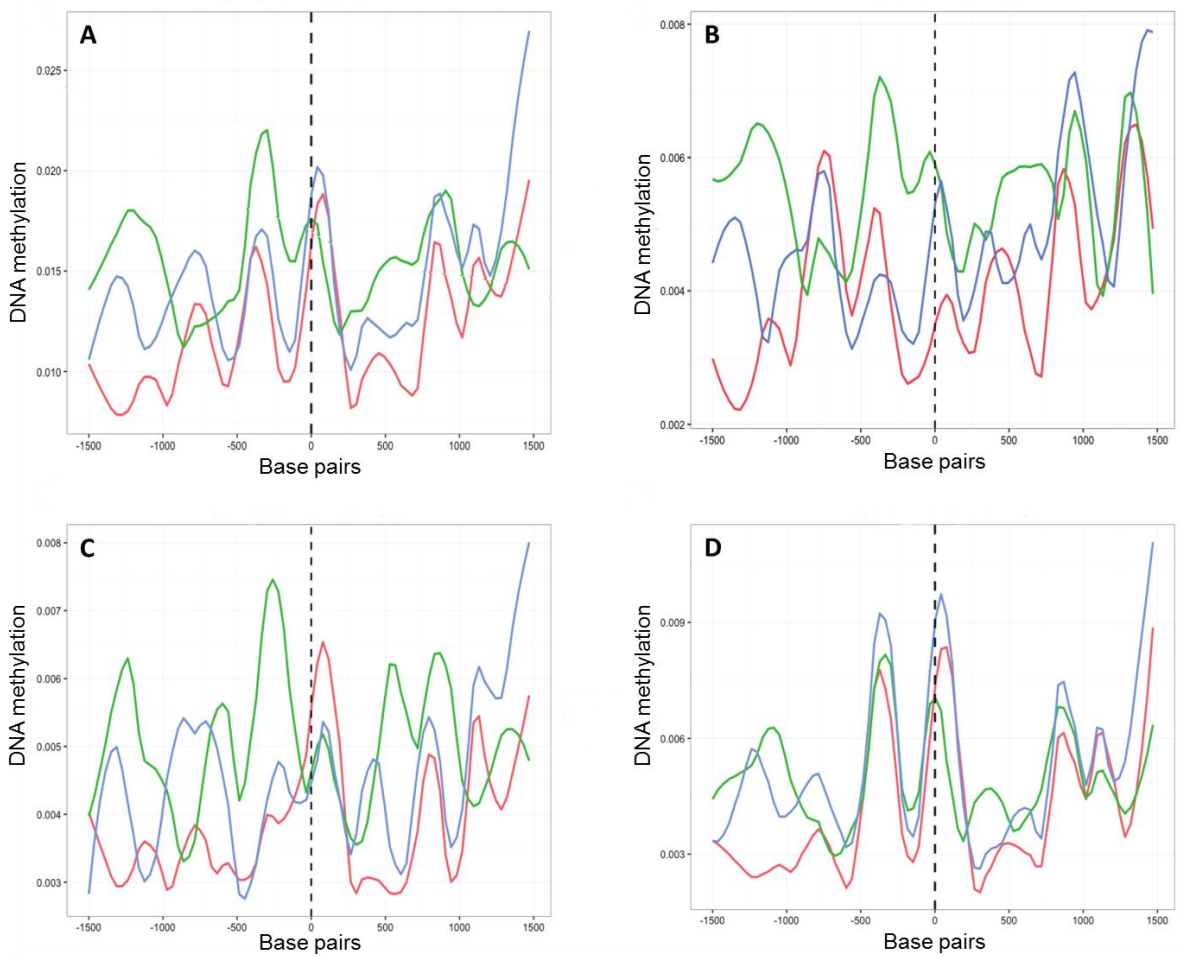

Figure 5: Methylation density across transcription start sites (TSS) found in 131 genes associated to polysaccharide degradation in *B. cinerea* (27). Methylation level (Vertical axis) at each time point (T1, red; T8, green and T8P, blue) was identified as the proportion of methylated cytosines against all cytosines in 30bp windows 1.5kb before and after the transcription start site (TSS) (Horizontal axis). **A)** Methylation level for all mCs; **B)** Methylation level for CpG context; **C)** Methylation level for CpHpG context and **D)** Methylation level for CpHpH context.

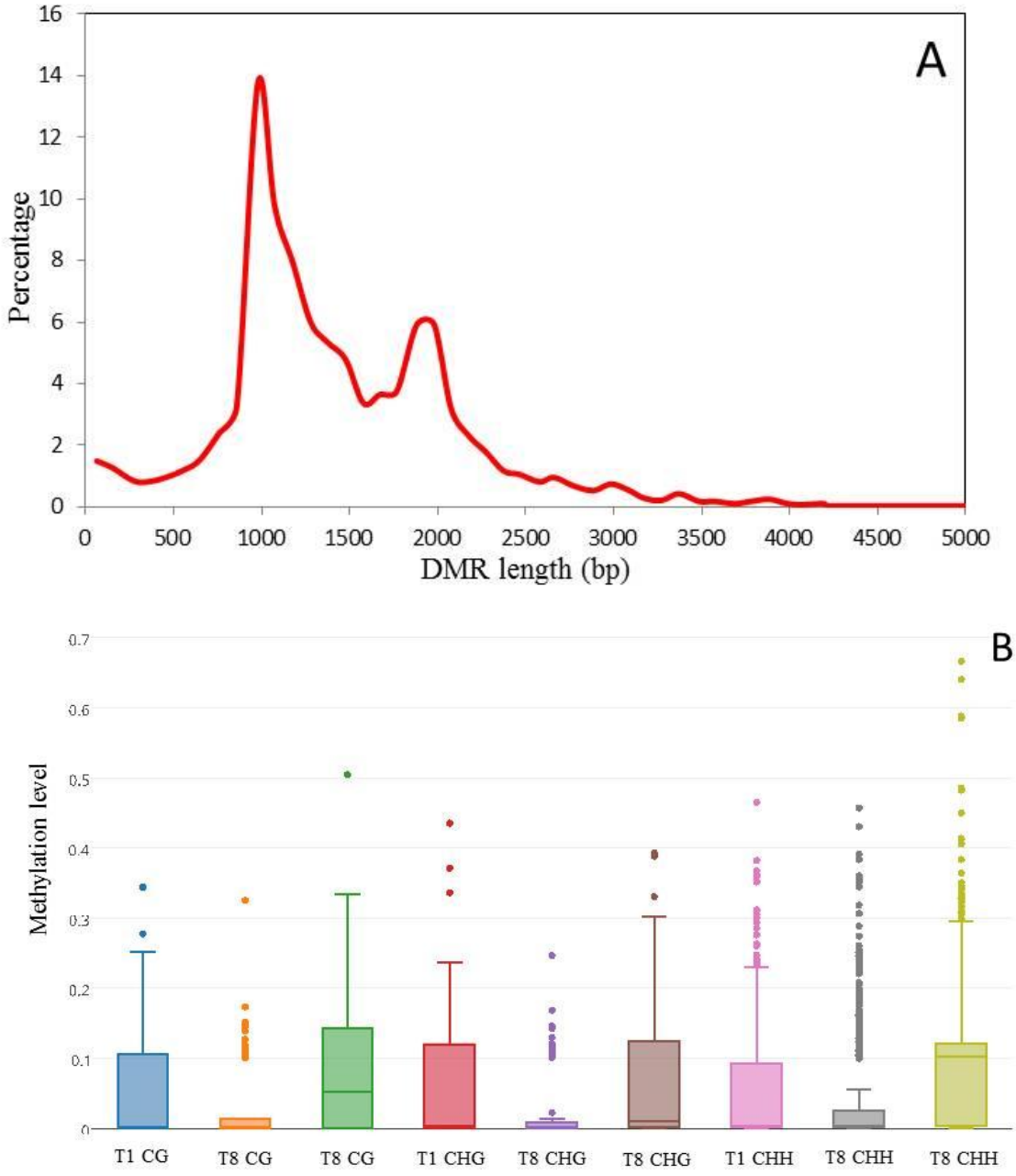

Figure 6: Analysis of *in vitro* culture induced DMRs in *Botrytis cinerea*. (a) Length distribution of *in vitro* culture induced DMRs in *Botrytis cinerea*. DRMs (i.e., regions presenting significantly different methylation levels between one sample and the other two samples (FDR<0.01)) were determined using a three sample Kruskal-Wallis test. Methylation levels were analysed by sliding window analysis using swDMR. DMRs were determined for all cytosines. **(b)** Methylation level distribution in *in vitro* induced DMRs. Boxplot of 3 sample sliding window differential methylation analysis using swDMR. The boxplots shows

840 the distribution of each methylation in each context (CG, CHG and CHH) at three time points

841 (T1, T8 and T8P), circles indicate DMRs with outlier levels of methylation.

842

Table 1: *Botrytis cinerea* virulence genes with known function overlapping with *in vitro* culture induced DMRs. Columns Gene Variant and Gene/DMR overlap indicate the number (#) and percentage (%) of genes in each functional group with a genetic variant or overlapping with a Differentially Methylated Region respectively. Column DMR type indicate how methylation levels changed when comparing all three samples (T1, T8 and T8P). DMRs were grouped according to their changing patterns into recovery (T1=T8P) and non-recovery (T1< > T8P). Two subgroups where found for recovery (T1=T8P < T8 (Type 0) and T1=T8P > T8 (Type 2)) and non-recovery (T1>T8=T8P (Type 1a) and T1=T8<T8P (Type 1b)). Virul. s.l. indicates virulence genes in abroad sense and include genes associated to: Appressorium formation, virulence on a strict sense and CAZyme genes. (1,2)(26,27)

Gene Function		Total	Gene Variant		Gene/DMR overlap		DMR Type				Reference
			#G/D	%G/D	#G/D	%G/D	Recovery		Non-recov		
							0	2	1a	1b	
Housekeeping		5	-	-	-	-	-	-	-	-	(26)
Apoptosis		10	2	20	4	40.0	3	1	-	-	(26)
Conidiation		16	-	-	6	37.5	1	2	-	3	(26)
Mating and fruit body development		32	6	18.8	6	18.7	1	4	1	1	(26)
Secondary metabolism		51	4	7.8	14	27.5	9	3	2	3	(26)
Signalling pathways		176	6	3.4	54	30.7	12	17	7	20	(26)
Sclerotium formation		249	7	2.8	67	26.9	26	31	10	13	(26)
Virul. *s.l.*	Appressorium	12	2	16.7	3	25.0	1	-	-	3	(26)
	Virulence *s.s.*	17	1	5.9	4	23.5	1	1	1	2	(27)
	CAZyme genes	1155	50	4.3	320	27.7	112	132	45	99	(28)
Total		**1577**	**68**	**4.3**	**478**	**30.3**	**166**	**191**	**66**	**144**	

855 **Table 2: Number of Differentially Methylated Regions (DMRs) between T1, T8 and T8P**
856 **samples.** DRMs (i.e., regions presenting significantly different methylation levels between
857 one sample and the other two samples (FDR<0.01)) were determined using a three sample
858 Kruskal-Wallis test. Methylation levels were analysed by sliding window analysis using
859 swDMR. DMRs were determined for all cytosines and for three methylation contexts. DMRs
860 were grouped according to their changing patterns into recovery (T1=T8P) and non-recovery
861 (T1< > T8P). Two subgroups where found for recovery (T1=T8P < T8 (Type 0) and T1=T8P
862 > T8 (Type 2)) and non-recovery (T1>T8=T8P (Type 1a) and T1=T8<T8P (Type 1b)).
863 Percentage of the total DMRs for each pattern type/sequence context is shown in parenthesis.
864

	Total	Recovery (%)		Total recovery (%)	No recovery	
		Type 0	Type 2		In vitro induced (Type 1a)	Plant induced (Type 1b)
mC	2822	757 (26.82)	860 (30.47)	1617 (57.30)	452 (16.02)	753 (26.68)
CG	70	17 (24.29)	15 (21.43)	32 (45.71)	14 (20.00)	24 (34.29)
CHG	82	14 (17.07)	30 (36.59)	44 (53.66)	15 (18.29)	23 (28.05)
CHH	1248	303 (24.28)	490 (39.26)	793 (63.54)	137 (10.98))	318 (25.48)
Total	4222	1395 (33.04)	1091 (25.84)	2486(58.88)	618 (14.64)	1118 (26.48)

865
866

867 **Table 3: *Botrytis cinerea in vitro* induced Differentially Methylated Regions overlapping**
868 **with genes.** DRMs overlapping with genes (i.e., regions presenting significantly different
869 methylation levels between one sample and the other two samples (FDR<0.01)) were
870 determined using a three sample Kruskal-Wallis test. Methylation levels were analyzed by
871 sliding window analysis using swDMR. DMRs were determined for all cytosines and for
872 three methylation contexts. DMRs were grouped according to the genic region they
873 overlapped with (i.e, Promoter, promoter and Gene body, promoter, Gene body and 3'UTR,
874 gene body and 3'UTR and gene body). (**) Percentage of the total DMRs overlapping with
875 each particular genic region. (*) Percentage of the total number of genes showing a
876 methylation recovery pattern.

877

	Total genes	Promoter, Gene body and 3'UTR (*)	Promoter only (*)	Promoter and Gene body (*)	Gene body and 3'UTR (*)	Gene body (*)
mC	3055	626 (20.49)	61 (2.00)	1022 (33.45)	923 (30.21)	423 (13.85)
CG	68	3 (4.41)	0 (0.00)	24 (35.29)	21 (30.88)	20 (29.41)
CHG	84	8 (9.52)	0 (0.00)	29 (34.52)	27 (32.14)	20 (23.81)
CHH	1339	248 (18.52)	32 (2.39)	443 (33.08)	413 (30.84)	203 (15.16)
	Recovery genes (**)					
mC	1713 (56.07)	345 (20.14)	43 (2.51)	545 (31.82)	537 (31.35)	243 (14.19)
CG	32 (47.06)	2 (6.25)	0 (0.00)	11 (34.38)	9 (28.13)	10 (31.25)
CHG	46 (54.76)	4 (8.70)	1 (2.17)	13 (28.26)	16 (34.78)	12 (26.09)
CHH	863 (64.45)	175 (20.28)	21 (2.43)	286 (33.14)	252 (29.20)	129 (14.95)

878
879
880
881

Supplementary Tables

Supplementary Table 2: Average coverage statistics for Whole Genome Bisulfite Sequenced samples. Average measurements were obtained from three replicates at each time point. Sequencing reads from all samples were mapped to *B. ciniera* B05.10 genome using Bismark/Bowtie2.

Sample	Mean Coverage	Std dev	Cytosine coverage	Cytosine coverage (>4x)	mC (>1x)
T1	54.9939	20.3428	92.55%	87.65%	10.99%
T8	33.1991	13.868	91.50%	81.07%	9.14%
T8P	45.0209	17.0144	93.42%	86.67%	10.63%

Supplementary Table 3: Genome mapping statistics from 9 bisulfite converted Botrytis samples. Sequencing reads from all samples were mapped to *B. ciniera* B05.10 genome using Bismark/Bowtie2

			Total methylated C's			Total non-methylated C's			% methylation			%mC
Samples	Total bp	% Map. Effic	CpG	CHG	CHH	CpG	CHG	CHH	CpG	CHG	CHH	
T1BS1	26382612	67.6	477254	438983	2499975	130600424	111869938	391807290	0.36	0.39	0.63	0.54
T1BS2	34048060	62.9	526341	485477	2494454	155155501	134341879	485255169	0.34	0.36	0.51	0.45
T1BS3	17347608	61.1	306505	279816	1575956	77226256	66054702	232502707	0.40	0.42	0.67	0.57
AvT1	25926093.33	63.87	436700.00	401425.33	2190128.33	120994060.33	104088839.67	369855055.33	0.36	0.38	0.59	0.52
T8BS1	18543427	62	394348	360641	1568745	83351098	71894819	257263175	0.47	0.50	0.61	0.56
T8BS2	12613134	60.7	248968	229853	902624	55786373	47759672	166229028	0.44	0.48	0.54	0.51
T8BS3	17117307	65.1	391446	360065	2142019	79537475	69135859	257486354	0.49	0.52	0.83	0.71
AvT8	16091289.33	62.60	344920.67	316853.00	1537796.00	72891648.67	62930116.67	226992852.33	0.47	0.50	0.67	0.59
T8PBS1	28336888	62.3	524875	487874	3561078	126943754	110309124	404488048	0.41	0.44	0.87	0.71
T8PBS2	18471780	66.9	435528	403984	2932991	89352607	77332840	279892313	0.49	0.52	1.04	0.84
T8PBS3	14694194	54.3	220458	201667	924438	57483914	49293008	173794940	0.38	0.41	0.53	0.48
AvT8P	20500954.00	61.17	393620.33	364508.33	2472835.67	91260091.67	78978324.00	286058433.67	0.43	0.46	0.86	0.68

902

903 **Supplementary Table 8:** Primer sequences used for MSAP.

Oligo name	Function	Sequence
Ad *Hpa*II/*Msp*I	Reverse Adaptor	GACGATGAGTCTAGAA
Ad. *Hpa*II/*Msp*I	Forward Adaptor	CGTTCT AGACTCATC
Ad. *EcoR*I	Reverse Adaptor	AATTGGTACGCAGTCTAC
Ad *EcoR*I	Forward Adaptor	CTCGTAGACTGCGTACC
Pre. *EcoR*I	Preselective primer	GACTGCGTACCAATTCA
Pre. *Hpa*II/*Msp*I	Preselective primer	GATGAGTCCTGAGCGGC
*EcoR*I2	Selective primer	GACTGCGTACCAATTCAAC
*Hpa*II 2.1	Selective primer	GATGAGTCCTGAGCGGCA

904
905
906
907

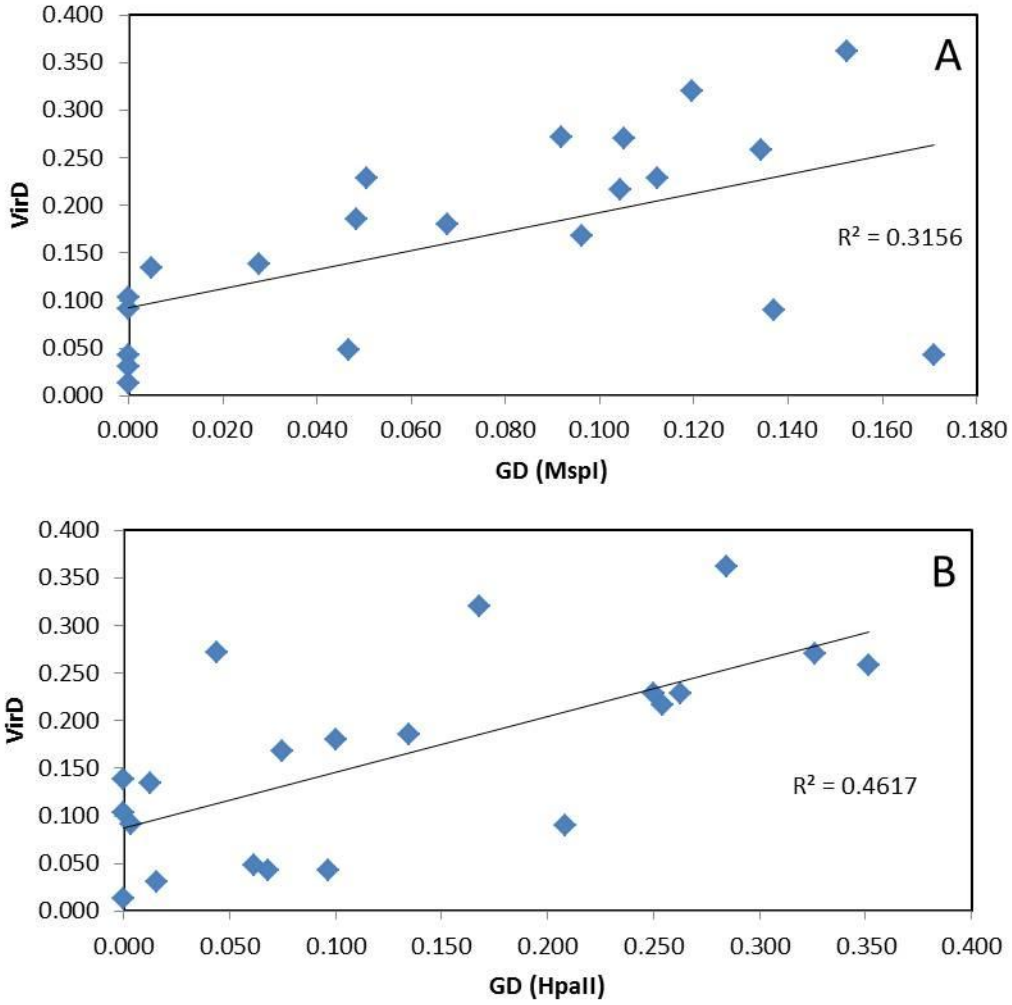

Figure S1: Correlation between pairwise molecular differentiation and changes in virulence observed during *in vitro culture* of *B. cinerea*. Correlations were calculated using mantle test analysis on pairwise PhiPT values **(GD)** (generated from MSAP data obtained using MspI **(A)** and HpaII **(B)**) and differences in virulence between culture time points **(VirD)**. Analysis using 1000 permutations showed significant correlations (**A**: P = 0.005; **B**: P = 0.002).

922

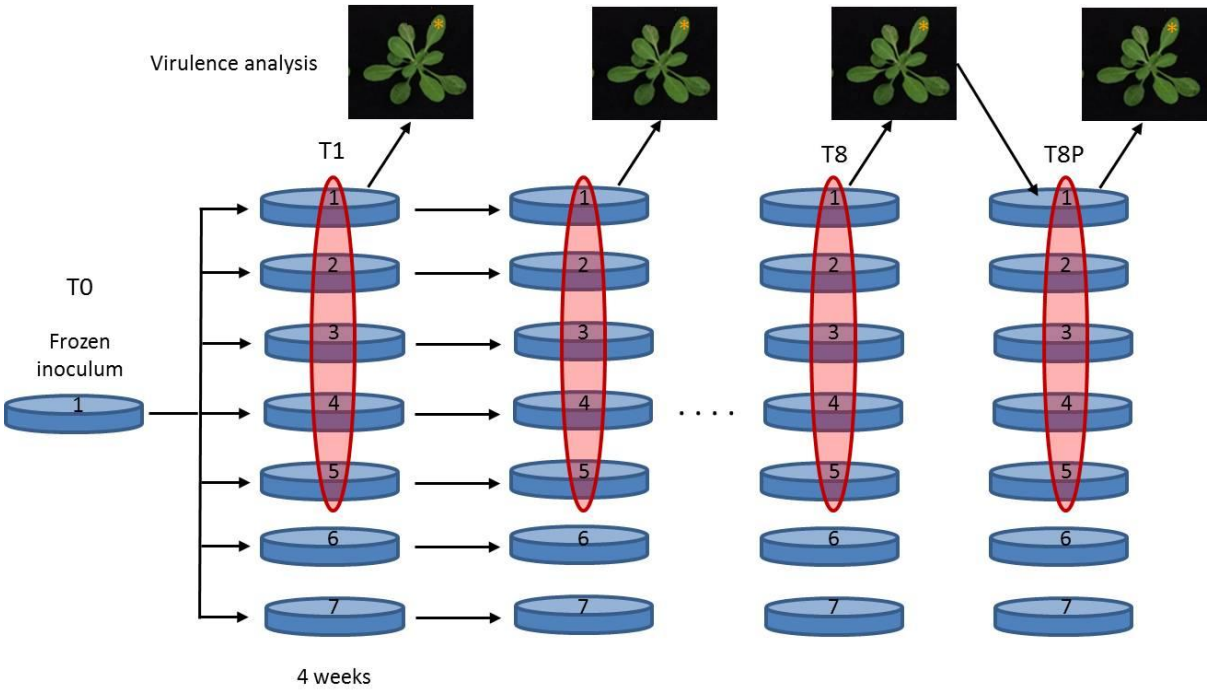

Figure S2: Schematic representation of experimental design. Seven replicated *Botrytis cinerea* cultures were initiated from a single frozen inoculum and cultured for 36 weeks. All replicates were subcultured every 4 weeks to fresh culture medium and mycelia were kept for DNA analysis (MSAPs, WGS, and BS-WGS). Conidia from five randomly selected replicates (highlighted in red) at each time point were collected and used for virulence analysis by inoculating five *Arabidopsis thaliana*. Inoculated *A. thaliana* leaves* at T1, T8 and T8P were collected 72 hours after inoculation for estimation of *in planta* fungal development by quantitative PCR. Conidia from were collected from *A. thaliana* tissue infected with T8 fungus and were re-cultured for a short time to generate conidia to test virulence recovery.